

Synthesis and Characterization of Graphene-ZnO Nanocomposite and its Application in Photovoltaic Cells

F. S. Ghoreishi^a, V. Ahmadi^{b,*}, M. Samadpour^c

^a Dept. of Nanotechnology Engineering, Tarbiat Modares University, Tehran, Iran

^b Dept. of Electrical & Computer Engineering, Tarbiat Modares University, Tehran, Iran

^c Dept. of Physics, K.N.Toosi University of Technology, Tehran, Iran

Article history:

Received 6/10/2013

Accepted 25/12/2013

Published online 1/3/2014

Keywords:

Nanocomposite

Graphene

ZnO

Photovoltaic cell

CdS

Abstract

In this paper, we present a simple method for preparation of graphene-ZnO nanocomposites (G-ZnO). The method is based on thermal treatment of the graphene oxide (GO)/ZnO paste which reduces the graphene oxide into the graphene and leads to the formation of the G-ZnO nanocomposite. The structure, morphology and optical properties of synthesized nanocomposites are characterized with XRD, FESEM, FTIR and Raman spectroscopies. Here CdS quantum dots are deposited on G-ZnO nanocomposite structure and is integrated as a photoanode in CdS quantum dot sensitized solar cells (QDSSCs). Photovoltaic properties of CdS QDSSC based on bare ZnO nanoparticles and G-ZnO nanocomposite photoanodes are studied here. The cell with G-ZnO/CdS photoanode shows two times higher photoelectric conversion efficiency than that of the pure ZnO photoanode (0.94 vs. 0.45).

2014 JNS All rights reserved

1. Introduction

Graphene, a single 2D carbon sheet, has recently attracted great attention because of its remarkable properties such as high surface area, high chemical stability and unique electronic properties especially ultrahigh electron mobility [1, 2]. These excellent features qualify graphene as an ideal candidate for many applications such as optoelectronic devices [3], batteries [4] and nanocomposites [5]. It is

shown that incorporation of graphene into the ceramic [6] or polymer [7, 8] matrices, improves the features of these host materials. Recently graphene/inorganic nanocomposites originated from the decoration of graphene sheets with inorganic nanoparticles such as metal, metal oxide and sulfide, are attracting a great interest. Until now, various graphene/inorganic nanocomposites have been

synthesized and shown favorable properties that are not found in the separate components [9, 10].

ZnO semiconductor with different morphologies, wide band gap (3.37 eV) and large exciton binding energy (60 meV), have many potential applications in photocatalysis [11], transistors [6, 12], sensors [13], and solar cells [14]. The optical properties of ZnO nanoparticles play an important role in optoelectronic, catalytic and photochemical properties [15, 16].

Quantum-dot-sensitized solar cells (QDSSCs) have been explored as one of the most promising candidates for third-generation photovoltaic devices [17]. Quantum dots have specific benefits such as size dependent band gaps, high extinction coefficient and ability of multiple exciton generation [18, 19], in comparison with dyes. The main disadvantage in QDSSCs is charge recombination at the interface of photoanode layer and electrolyte [20-22]. So, preventing charge recombination at the photoanode layer-electrolyte interface is a key factor to improve the performance of QDSSCs. Graphene with high electron mobility can increase the charge transport in the cell and thus reduces charge recombination at the photoanode interface.

In this study, we present a simple method for synthesizing G-ZnO nanocomposite with low cost and easily available precursors and explore its structure, optical and photovoltaic properties. Photovoltaic characteristics of CdS QDSSCs with G-ZnO photoanodes are reported in comparison with cells with pure ZnO photoanodes. The conversion efficiency of cells with G-ZnO photoanode is improved 100% in comparison with cells without graphene sheets.

2. Experimental procedure

The G-ZnO nanocomposite is prepared as follows. The Graphene oxide (GO) is first prepared from

graphite fine powder (Merck chemical) by the Hummer's method [23]. Also the ZnO nanoparticles are synthesized by precipitation method as described by Chen et al. [24]. Then, 5 g ZnO powder, 22 mg GO, 29 mL ethyl cellulose (ethoxyl basis, Aldrich) ethanolic solution (10 wt. %) and 22 mL terpineol ($\geq 95\%$, Fluka) are mixed together and sonicated for 10 minutes. Finally the GO-ZnO paste is obtained after heating the mixture in the rotary evaporator and removing the residual ethanol in it. The paste is deposited on fluorine doped tin oxide (FTO) substrate (glass/FTO 8Ω , Dyesol Co.) by doctor-blading method to make a thin film and annealed at $550 \text{ }^\circ\text{C}$ for 60 min. The annealing process reduces the GO into the graphene (partially reduced graphene oxide) and also removes the residual precursors from the G-ZnO nanocomposite (theoretical model predicted that the complete reduction may be difficult [25]). Similar procedure is employed to obtain ZnO coated FTO substrate.

For investigating the photovoltaic properties of the synthesized nanocomposite and comparing it with ZnO layer, QDSSCs with CdS sensitizers have been fabricated based on ZnO and G-ZnO nanocomposite photoanodes. For this purpose, the ZnO and G-ZnO photoelectrodes, are sensitized with CdS quantum dots by the successive ionic layer adsorption and reaction (SILAR) method [26]. The polysulfide electrolyte [27] and Cu_2S counter electrodes [28], have been used for solar cell fabrication.

Photocurrent-voltage (I-V) characteristics are recorded at a range of air mass 1.5G illumination intensity using a solar simulator (SIM-10-2, SHARIF SOLAR).

The synthesized materials and samples are characterized by Field emission scanning electron microscopy (FESEM, XL30 Philips), a powder X-ray diffraction system (XRD, X'Pert, Philips, $\text{Cu K}\alpha$

, $\lambda_0=1.540 \text{ \AA}$), Fourier transform infrared (FTIR) spectroscopy (Frontier FTIR equipment, Perkin Elmer) and Raman spectroscopy (SENTERRA Raman spectrometer, BRUKER). Photocurrent–voltage (I–V) characteristics are recorded by using a solar simulator at a range of air mass 1.5G illumination intensity (SIM-10-2, SHARIF SOLAR).

3. Results and discussion

The XRD spectra for the ZnO nanoparticles and the G-ZnO nanocomposites are shown in the Fig. 1. The peak pattern for ZnO, matches with the JCPDS (65-3411) data for a wurtzite hexagonal structure [29]. The average size of 50 nm is achieved for ZnO nanocrystals from Debye–Scherrer formula [30]. GO has a diffraction peak centered at $2\theta = 10.8^\circ$ related to (001) but this peak is not observed in the XRD pattern of G-ZnO nanocomposite. However, for G-ZnO nanocomposite a new weak and broad diffraction peak around at $2\theta = 26^\circ$ appears, indicating the reduction of GO into the graphene and the disordered stacking of graphene sheets in the nanocomposite [31-33]. The graphene diffraction peak located at $2\theta = 26^\circ$ which is related to (002), is much weaker than ZnO peaks due to the small mass ratio of graphene in comparison with ZnO. This analysis clearly indicates the formation of graphene sheets which are decorated by hexagonal ZnO nanoparticles.

The morphological characterizations of ZnO nanoparticles and GO sheets are carried out using FESEM. Fig. 2(a) shows the FESEM image of pure ZnO nanoparticles synthesized by precipitation method. As can be seen, the ZnO nanoparticles have quasi-spherical shapes and their average size is in the range of 50 nm. This average size obtained by FESEM image is in good agreement with the approximate size calculated from Debye–Scherrer

formula. Fig. 2(b) shows a layered structure of as prepared GO nanosheets. It is clearly observed that the sheets are tending to restack to each other.

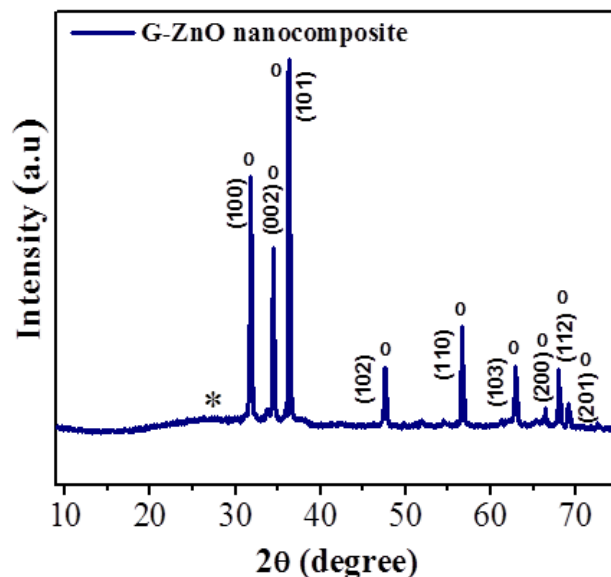


Fig. 1. XRD patterns of the G-ZnO nanocomposite. \bullet and * represent diffraction peaks belonging to ZnO and graphene, respectively.

The Raman spectra of GO and G-ZnO nanocomposite are shown in Fig. 3. Both samples exhibit two peaks named D-band and G-band. The D-band is related to the disordered carbon and the G-band is associated with the in-plane stretching vibration of sp^2 C–C bonds [34]. The I_D/I_G ratio increases from 1.2 in GO to 1.4 in G-ZnO due to the removal of oxygen functional groups upon reduction of GO, decrement of the size of the sp^2 domains formed in the graphene and interaction between graphene sheets and ZnO nanoparticles [35].

Fig. 4 shows the FTIR spectra of the GO and G-ZnO nanocomposite. The oxygen functional group peaks in GO are centered at 1071, 1178 and 1730 cm^{-1} , which correspond to the C–O stretching vibrations, C–O–H deformation vibrations and C=O stretching of COOH groups, respectively.

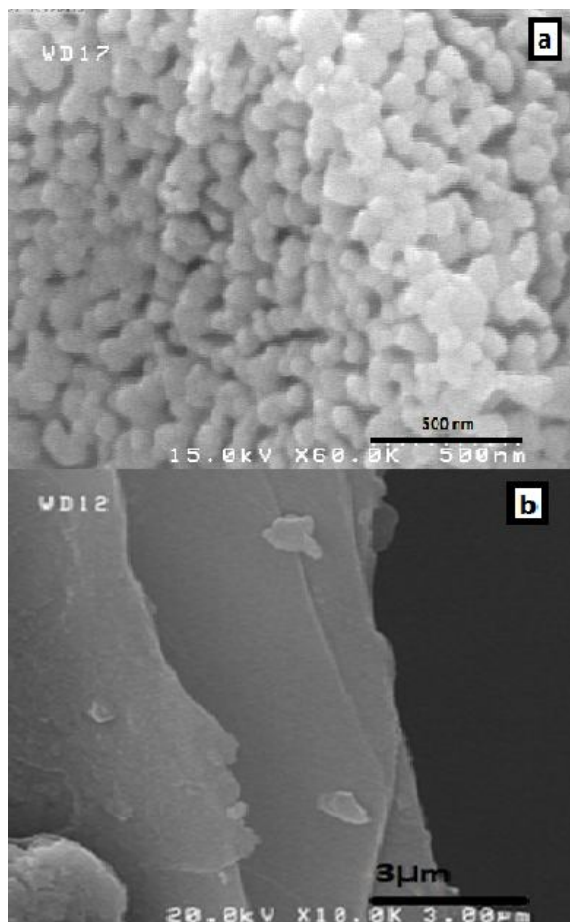


Fig. 2. FESEM images of synthesized (a) ZnO nanoparticles and (b) graphene oxide sheets

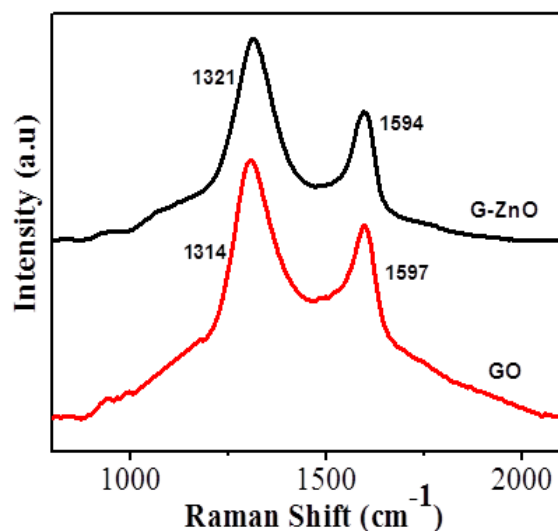


Fig. 3. Raman spectra of GO and G-ZnO nanocomposite.

The peak at 1615 cm^{-1} can be attributed to the skeletal vibrations of unoxidized graphitic domains. The strong peak assigned to the stretching vibrations of the hydroxyl groups of GO appears at 3280 cm^{-1} [36]. However, all these bands related with the oxygen functional groups almost disappear or appear with significantly lower intensities in the FTIR spectra of the G-ZnO nanocomposites. These results confirm that these oxygen functional groups are almost removed in the process of thermal reduction, and the GO is reduced to a great extent. In the Fig. 4, the strong peak at 575 cm^{-1} is the characteristic peak of the Zn–O stretching vibration in ZnO nanoparticles [33].

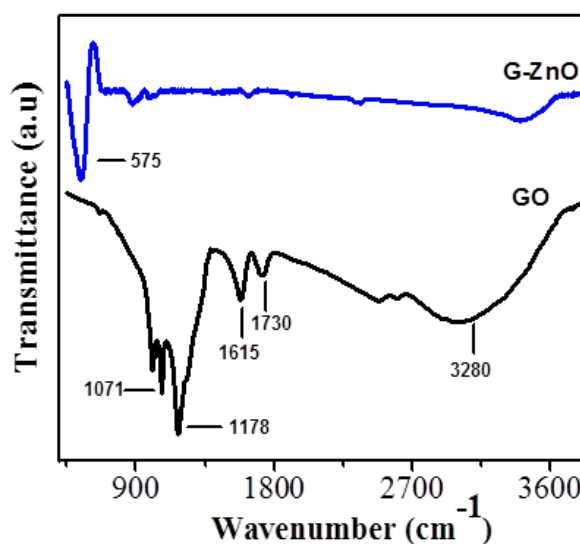


Fig. 4. FTIR spectra of GO and G-ZnO nanocomposite.

Fig. 5 shows the photocurrent density–voltage curves of the QDSSCs which are fabricated by ZnO and G-ZnO nanocomposites as photoanodes, under simulated $100\text{ mW}\cdot\text{cm}^{-2}$ illumination. The photovoltaic properties of both cells are shown in Table 1.

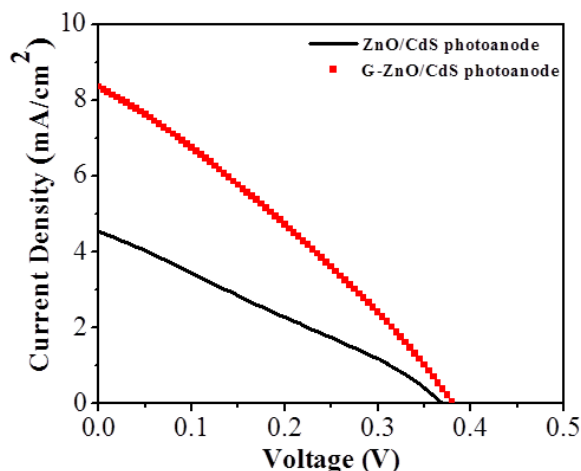


Fig. 5. I-V curves of ZnO and G-ZnO nanocomposite QDSSCs.

Table 1. Photovoltaic characteristics of the QDSSCs with ZnO/CdS and G-ZnO/CdS Photoanodes at 100 mW.cm^{-2} light intensity

Photoanode layer	J_{sc} (mA.cm^{-2})	V_{oc} (V)	FF	η (%)
ZnO/CdS	4.53	0.37	0.25	0.45
G-ZnO/CdS	8.35	0.38	0.29	0.94

The short circuit current density (J_{sc}), open circuit voltage (V_{oc}) and conversion efficiency (η) are achieved equal to 4.53 mA/cm^2 , 0.37 V and 0.45% , respectively for ZnO based cell while the cell with G-ZnO nanocomposite photoanode, exhibits J_{sc} , V_{oc} and η of 8.35 mA/cm^2 , 0.38 V and 0.94% , respectively. According to Table 1, while the V_{oc} is almost the same in both cells, the J_{sc} of the cell with G-ZnO photoanode is significantly enhanced about twice in comparison with the J_{sc} of the cell with ZnO photoanode. This considerable enhancement of the J_{sc} and efficiency of the cell with G-ZnO nanocomposite, is because of the unique properties of graphene. Ultrahigh electron mobility in graphene, increases the electron transfer rate at the interface of photoanode and electrolyte, and leads in lower recombination rate at the interface and thus

improving the conversion efficiency of QDSSCs [37].

4. Conclusion

In the present work, G-ZnO nanocomposite has been synthesized by a simple method of thermal treatment of GO-ZnO paste. Thermal treatment, partially reduced GO into the graphene and also resulted in the pure G-ZnO nanocomposite without any residual precursors. The XRD analysis indicated the formation of graphene decorated by hexagonal ZnO nanoparticles with average size of 50 nm . FTIR and Raman spectra clearly confirmed the thermal reduction of graphene oxide and thus the formation of G-ZnO nanocomposite. QDSSCs fabricated with ZnO and G-ZnO photoanodes were assembled and tested under 1 sun illumination. The cells with nanocomposite photoanodes showed 100% improvement in the conversion efficiency in comparison with the cells based on bare ZnO photoanodes. Also a significant enhancement in the short circuit current density was observed in the cells with G-ZnO photoanodes as compared to the ones with ZnO nanoparticles. This enhancement is related to the increase of the electron transfer rate in the G-ZnO nanocomposite photoanode which is originated from the ultrahigh electron mobility of graphene sheets. Therefore it is concluded that G-ZnO nanocomposite could be a promising candidate for better photovoltaic performance in QDSSCs.

References

- [1] Y. Zhu, S. Murali, W. Cai, X. Li, J.W. Suk, J.R. Potts, R.S. Ruoff, *Adv. Mater.* 22 (2010) 3906-3924.
- [2] J. Wu, W. Pisula, K. Müllen, *Chem. Rev.* 107 (2007) 718-747.
- [3] F. Bonaccorso, Z. Sun, T. Hasan, A. Ferrari, *Nature Photon.* 4 (2010) 611-622.

- [4] Y. Wang, Z.S. Feng, J.J. Chen, C. Zhang, *Mater. Lett.* 71 (2012) 54-56.
- [5] Q. Li, B. Guo, J. Yu, J. Ran, B. Zhang, H. Yan, J.R. Gong, *J. Am. Chem. Soc.* 133 (2011) 10878-10884.
- [6] S. Watcharotone, D.A. Dikin, S. Stankovich, R. Piner, I. Jung, G.H. Dommett, G. Evmenenko, S.-E. Wu, S. F. Chen, C. P. Liu, *Nano Letters* 7 (2007) 1888-1892.
- [7] S. Stankovich, D.A. Dikin, G.H. Dommett, K.M. Kohlhaas, E.J. Zimney, E.A. Stach, R.D. Piner, S.T. Nguyen, R.S. Ruoff, *Nature* 442 (2006) 282-286.
- [8] G. Eda, M. Chhowalla, *Nano Lett.* 9 (2009) 814-818.
- [9] C. Xu, X. Wang, J. Zhu, X. Yang, L. Lu, J. Mater. Chem. 18 (2008) 5625-5629.
- [10] G. Williams, P.V. Kamat, *Langmuir* 25 (2009) 13869-13873.
- [11] V. Houšková, V. Štengl, S. Bakardjieva, N. Murafa, A. Kalendová, F. Opluštil, *J. Phys. Chem. A* 111 (2007) 4215-4221.
- [12] Y. Li, G. Meng, L. Zhang, F. Phillipp, *Appl. Phys. Lett.* 76 (2000) 2011-2013.
- [13] J. Goldberger, D.J. Sirbully, M. Law, P. Yang, *J. Phys. Chem. B* 109 (2005) 9-14.
- [14] Q. Zhang, C.S. Dandeneau, X. Zhou, G. Cao, *Adv. Mater.* 21 (2009) 4087-4108.
- [15] N. Goswami, D.K. Sharma, *Physica E* 42 (2010) 1675-1682.
- [16] C. Feldmann, *Adv. Funct. Mater.* 13 (2003) 101-107.
- [17] P.V. Kamat, *J. Phys. Chem. C* 112 (2008) 18737-18753.
- [18] R.J. Ellingson, M.C. Beard, J.C. Johnson, P. Yu, O.I. Micic, A.J. Nozik, A. Shabaev, A.L. Efros, *Nano Lett.* 5 (2005) 865-871.
- [19] P.E.P.Q.E. Exceeding, *Octavi E* 1530-1533.
- [20] I. Mora-Seró, S. Gimenez, F. Fabregat-Santiago, R. Gomez, Q. Shen, T. Toyoda, J. Bisquert, *Acc. Chem. Res.* 42 (2009) 1848-1857.
- [21] I. Mora-Seró, J. Bisquert, *J. Phys. Chem. Lett.* 1 (2010) 3046-3052.
- [22] J. Kim, H. Choi, C. Nahm, J. Moon, C. Kim, S. Nam, D.R. Jung, B. Park, *J. Power Sources* 196 (2011) 10526-10531.
- [23] W.S. Hummers Jr, R.E. Offeman, *J. Am. Chem. Soc.* 80 (1958) 1339-1339.
- [24] C. Chen, P. Liu, C. Lu, *Chem. Eng. J.* 144 (2008) 509-513.
- [25] D. Boukhvalov, M. Katsnelson, *Phys. Rev. B* 78 (2008) 1320-1325.
- [26] Y. Chen, Y. Zhang, W. Fu, H. Yang, Q. Tao, Y. Zhang, S. Su, P. Wang, M. Li, *Electrochim. Acta* (2013) 647-652.
- [27] V. Jovanovski, V. González-Pedro, S. Giménez, E. Azaceta, G.n. Cabañero, H. Grande, R. Tena-Zaera, I.n. Mora-Seró, J. Bisquert, *J. Am. Chem. Soc.* 133 (2011) 20156-20159.
- [28] Z. Yang, C.Y. Chen, C.W. Liu, C.L. Li, H.T. Chang, *Adv. Energy Mater.* 1 (2011) 259-264.
- [29] C. Zhang, J. Zhang, Y. Su, M. Xu, Z. Yang, Y. Zhang, *Physica E* 56 (2014) 251-255.
- [30] C. He, T. Sasaki, Y. Shimizu, N. Koshizaki, *Appl. Surf. Sci.* 254 (2008) 2196-2202.
- [31] B. Li, H. Cao, *J. Mater. Chem.* 21 (2011) 3346-3349.
- [32] D. Cai, M. Song, *J. Mater. Chem.* 17 (2007) 3678-3680.
- [33] B. Saravanakumar, R. Mohan, S.J. Kim, *Mater. Res. Bull.* 48 (2013) 878-883.
- [34] B.N. Joshi, H. Yoon, S.H. Na, J.Y. Choi, S.S. Yoon, *Ceram. Int.* 40 (2014) 3647-3654.
- [35] Y.Z. Liu, Y.F. Li, Y.G. Yang, Y.F. Wen, M.Z. Wang, *Scripta Mater.* 68 (2013) 301-304.

- [36] M. Ahmad, E. Ahmed, Z. Hong, N. Khalid, W. Ahmed, A. Elhissi, J. Alloys Compd. 577 (2013) 717-727.
- [37] C.H. Hsu, J.R. Wu, L.C. Chen, P.S. Chan, C.C. Chen, Adv. Mater. Sci. Eng. 14 (2014) 312-316.